

# Thesis Title

*A subtitle of your thesis*

Author name



Thesis submitted for the degree of  
Master in Master's Program Name <change at  
main.tex>  
60 credits

Department Name <change at main.tex>  
Faculty name <change in duoforside.tex>

UNIVERSITY OF OSLO

Spring 2022



# Thesis Title

*A subtitle of your thesis*

Author name

© 2022 Author name

Thesis Title

<http://www.duo.uio.no/>

Printed: Reprosentralen, University of Oslo

# **Abstract**

# Contents

<b>1</b>	<b>Introduction</b>	<b>1</b>
<b>I</b>	<b>Theory</b>	<b>3</b>
<b>2</b>	<b>High-Entropy alloys</b>	<b>4</b>
2.1	Fundamentals . . . . .	4
2.2	Core effects and properties . . . . .	7
<b>3</b>	<b>Modeling of random alloys</b>	<b>9</b>
3.1	The Special Quasi-random Structure model . . . . .	9
3.1.1	Mathematical description . . . . .	10
3.1.2	Applications to high-entropy alloys . . . . .	12
<b>4</b>	<b>Density Functional Theory</b>	<b>16</b>
4.1	Review of Quantum Mechanics . . . . .	17
4.1.1	The Shrodinger equation . . . . .	17
4.1.2	Approximations to the many-body Shrodinger equation . . . . .	18
4.2	Kohn-Sham density functional theory . . . . .	20
4.2.1	Density functional theory . . . . .	20
4.2.2	The Kohn-Sham Equation . . . . .	21
4.3	Limitations of DFT - Insert refs . . . . .	22
<b>II</b>	<b>Methodology and Implementation</b>	<b>24</b>
<b>6</b>	<b>Practical application of DFT</b>	<b>23</b>
6.1	The Exchange-Correlation functional . . . . .	23
6.2	Fundamental aspects of practical DFT calculations . . . . .	24
6.3	Self-consistent field calculation . . . . .	26
<b>7</b>	<b>Computational details</b>	<b>28</b>
7.1	Vienna Ab initio Simulation Package . . . . .	28
7.2	Generation of SQS . . . . .	30
7.3	Figures . . . . .	31
7.3.1	Density of states . . . . .	31
7.3.2	Probability distribution functions . . . . .	31

7.3.3	Charge density . . . . .	31
7.4	Band gap . . . . .	31
7.5	Utility scripts . . . . .	31
<b>III</b>	<b>Results and Discussion</b>	<b>33</b>
<b>8</b>	<b>The results of (CrFeMnNi)Si<sub>2</sub> in the <math>\beta</math>-FeSi<sub>2</sub> structure</b>	<b>33</b>
8.1	Eqvimolar SQSs . . . . .	33
8.1.1	Introduction . . . . .	33
8.1.2	The band gap . . . . .	34
8.1.3	Local and Projected density of states . . . . .	36
8.1.4	Meta-GGA and hybrid functional . . . . .	40
8.1.5	Probability distribution functions and charge density	44
8.2	Permutations of the Cr <sub>4</sub> Fe <sub>4</sub> Mn <sub>4</sub> Ni <sub>4</sub> Si <sub>32</sub> high-entropy silicide	46
<b>9</b>	<b>Changing the elements</b>	<b>52</b>
<b>10</b>	<b>Overview and Relevance</b>	<b>57</b>
10.1	Cr <sub>4</sub> Fe <sub>4</sub> Mn <sub>4</sub> Ni <sub>4</sub> Si <sub>32</sub> in different crystal structures . . . . .	57
10.2	Overview . . . . .	59
<b>IV</b>	<b>Conclusion</b>	<b>60</b>
<b>A</b>	<b>Density of states</b>	<b>56</b>
<b>B</b>	<b>PDFs</b>	<b>57</b>
<b>C</b>	<b>Charge density</b>	<b>58</b>

# List of Figures

2.1	Formation of HEA based on $\delta$ and $N$ . Figures adopted from [14] . . . . .	6
2.2	A schematic illustration of lattice distortion in high-entropy alloys. Figure from [3] . . . . .	8
3.1	PDFs of (a) 20 and (b) 250 atom SQS models of CrFeMnNi [1] . . . . .	13
3.2	Density of states with SQS and MC/MD of FCC CoCrFeNi, figure from [1] . . . . .	14
3.3	Probability distribution functions with SQS and MC/MD of HCP CoOsReRu [1] . . . . .	14
4.1	Number of DFT studies per year from 1980 to 2021 [dimensions]. . . . .	16
6.1	Self consistent iteration of a DFT calculation. Figure adopted from lecture notes fys-mena4111 cite . . . . .	27
7.1	48 atom SQS based on eqvimolar distribution of Cr, Fe, Mn and Ni in and $FeSi_2$ cell. . . . .	32
8.1	Density of states SQS D CFMN (fesi2) from PBE calculation . . . . .	35
8.2	Density of states SQS B CFMN (fesi2) from PBE calculation . . . . .	36
8.3	Local density of states of Si (SQS D) . . . . .	37
8.4	Local density of states of TMs (SQS D), (a) Cr, (b) Mn, (c) Fe, (d) Ni . . . . .	37
8.5	Projected density of states SQS D CFMN (fesi2) from PBE calculation . . . . .	38
8.6	Projected density of states of SQS D and B around $E_F$ . . . . .	38
8.7	Density of states of SQS C with 2501 points vs 20000 points in the density of states. . . . .	39
8.8	Density of states of SQS E illustrating the different band gap from calculations with (a) PBE and (b) SCAN functional . . . . .	41
8.9	Total density of states of SQS (a) B and (b) E from calculations with HSE06 . . . . .	42
8.10	Probability distribution function of SQS D (top) and B (bottom) . . . . .	45
8.11	Charge density of SQS D and B from PBE calculations. Illustrated by VESTA . . . . .	46



8.12	Projected density of states of (a) $\text{Cr}_3\text{Fe}_3\text{Mn}_7\text{Ni}_3\text{Si}_{32}$ (SQS B), (b) $\text{Cr}_5\text{Fe}_5\text{Mn}_3\text{Ni}_3\text{Si}_{32}$ (SQS C), (c) $\text{Cr}_5\text{Fe}_3\text{Mn}_5\text{Ni}_3\text{Si}_{32}$ (SQS A), (d) $\text{Cr}_3\text{Fe}_5\text{Mn}_5\text{Ni}_3\text{Si}_{32}$ (SQS D) . . . . .	49
8.13	Density of states around $E_F$ of SQS D and E $\text{Cr}_5\text{Fe}_5\text{Mn}_3\text{Ni}_3\text{Si}_{32}$	50
8.14	Projected density of states of $\text{Cr}_3\text{Fe}_3\text{Mn}_3\text{Ni}_7\text{Si}_{32}$ around $E_F$ .	50
8.15	Probability distribution functions to $\text{Cr}_3\text{Fe}_5\text{Mn}_5\text{Ni}_3\text{Si}_{32}$ SQS D, <b>Maybe make larger</b> . . . . .	51
9.1	Projected density of states of $\text{Cr}_4\text{Fe}_4\text{Co}_4\text{Ni}_4\text{Si}_{32}$ . . . . .	54

# List of Tables

8.1	Total energy per atom, final magnetic moment, band gap (GGA) and formation enthalpy of $Cr_4Fe_4Mn_4Ni_4Si_{32}$ SQSs based on $FeSi_2$ . . . . .	34
8.2	Band gap transition of CFMN (fesi2) SQSs with PBE functional	35
8.3	Band gap (eV) with PBE in spin up and spin down channels of CFMN (fesi2) SQSs . . . . .	36
8.4	Band gap of CFMN ( $FeSi_2$ ) SQSs with GGA (PBE), meta-GGA (SCAN) and hybrid-functionals (HSE06). . . . .	40
8.5	Mean and stadard deviation of the total energy and magnetic moment per atom, plus enthalpy of formation of the listed mean energies ( $FeSi_2$ ). . . . .	47
8.6	Total and spin dependent band gap of 4 permutations of CFMN (fesi2) with PBE GGA calculation. The structures that are excluded from this list either failed in calculations, or does not show any band gap.< . . . . .	48
9.1	Summary of the total energy, enthalpy of formation and magnetization of several compositionally different SQS high-entropy alloys based on the $\beta$ - $FeSi_2$ unit cell. . . . .	52

# Preface

# Chapter 1

## Introduction

some introduction on the importance of discovering new materials and alloying.

**Need something on thermoelectricity related to both the band gap and high-entropy alloys.**

High-entropy alloys is a novel class of materials based on alloying multiple components, as opposed to the more traditional binary alloys. This results in an unprecedented opportunity for discovery of new materials with a superior degree of tuning for specific properties and applications. Recent research on high-entropy alloys have resulted in materials with exceedingly strong mechanical properties such as strength, corrosion and temperature resistance, etc **find references**. Meanwhile, the functional properties of high-entropy alloys is vastly unexplored. In this study, we attempt to broaden the knowledge of this field, the precise formulation of this thesis would be an exploration on the possibilities of semiconducting high-entropy alloys.

A key motivation of this thesis is the ability to perform such a broad study of complex materials in light of the advances in material informatics and computational methods. In this project, we will employ Ab initio methods backed by density functional theory on top-of the line supercomputers and software. 20 years ago, at the breaking point of these methods, this study would have been significantly narrower and less detailed firstly, but secondly would have totaled ... amount of CPU hours to complete (**Calculate this number**). In the addition to the development in computational power, is also the progress of modeling materials, specifically we will apply a method called Special Quasi-random Structures (SQS) to model high-entropy alloys or generally computationally complex structures. Together with the open landscape of high-entropy alloys described above, these factors produce a relevant study in the direction of applying modern computational methods to progress the research of a novel material class and point to promising directions for future research.

In specifics, this thesis revolve around the electrical properties of high-entropy alloys, mainly the band gap as this is the key indicator for a semiconducting material and it's applicability. Semiconductors are the building blocks in many different applications in today's world, ranging

from optical and electrical devices, to renewable energy sources such as solar and thermoelectricity. Given the economic and sustainable factors concerning silicon, in addition to its role in relevant applications such as microelectronics and solar power. Silicon emerges as a natural selection to build our alloys around. Furthermore, the development and research on both high entropy alloys and metal silicides have been heavily centered around 3d transition metals. Keeping in line with the economic and environmental factors, we will continue this direction by focusing on high entropy stabilized sustainable and economic 3d metal silicides **Not happy with this writing**. Throughout the study we will analyze a great number of permutations of 3d silicides, from different initial metal silicides such as  $CrSi_2$ ,  $FeSi_2$ ,  $MnSi_{1.75}$ ,  $Fe_2Si$ , each with distinct properties relating to the band gap, crystal structure and metal to silicon ratio. In addition, the permutations include numerous metal distributions and elements within the 3d-group of metals. Examples are Co, Cr, Fe, Mn, and Ni.

Given a background in high-entropy alloys, one could ask if this study is truly sensible. In the later sections we will cover the details of this field, and it quickly become clear that the materials investigated in this study does not fall under the precise definition of high-entropy alloys, nor do we intend to explore the properties and factors relating to high-entropy stabilized alloys such as the configurational entropy, phase stability and finite temperature studies. However this study is motivated from the discovery of these materials and promising properties, and venture into a more hypothetical space of materials, enabled by the computational methods available to study the potential properties of such materials. On the other hand, very recent studies **Mari, and other HEA silicide study** have experimentally synthesized high-entropy disilicides, thus in some way justifying the direction of this project.

We begin this project by reviewing key concepts of solid-state physics for readers lacking a background in materials science, and an introduction to the base 3d silicides of the experimental work. Later follows a theoretic walk-through of the relevant concepts of this thesis, these topics include high-entropy alloys, special quasi-random structures, and density functional theory. Next we shine light on the implementation of DFT in this project, and other computational details required to reproduce the results in this thesis, such as the use of the Vienna Ab Initio Simulation Package (VASP) and implementation of SQS. Finally we present the results of our study, these include the band gap and electronic properties of various structures and the success and challenges of the computational methods applied throughout the study.

# **Part I**

# **Theory**

## Chapter 2

# High-Entropy alloys

To begin this project, we give a brief description of high-entropy alloys (HEA). We introduce the basics and definitions, as well some more advanced topics relating to the functional properties of HEA's. This section will be largely based on the fantastic description of HEA's in "High-Entropy Alloys - Fundamentals and Application" and the references therein, it's an excellent read. This section is particularly based on chapters 1,2,3, and 7 [11], [14], [12], [13]

### 2.1 Fundamentals

High-Entropy Alloys are a quickly emerging field in materials science due to the infinitely many possibilities and the unique properties. From the original discovery by Jin in 2004, as of 2015 there have been over 1000 published journal articles on high-entropy alloys. In its simplicity, a high-entropy alloy can be compared to a smoothie. By combining an assortment of fresh fruit and vegetables one can produce unique combinations of flavors and nutritional values based on both the properties of the distinct items, and their interplay in the mixture. In materials science, this exact procedure can be applied to generate a large range of materials with tunable properties depending on the intended application. In the topic of HEA's, this can be increased strength or ductility, corrosive resistance or lowered thermal conductivity, all of which have been observed in actual high-entropy alloys. Moving on from the rather banal fruit analogy, a high-entropy alloy typically falls under the two conditions.

1. The material consist of at least 5 distinct elements, where each element contribute between 5-35% of the composition
2. The total configurational entropy is greater than  $1.5R$ , where  $R$  is the gas constant.

The latter is an especial case for high-entropy alloys. The ideal configurational entropy of random  $N$ -component solid-solution is given in eq 2.1

$$\Delta S_{\text{config}} = -R \sum_{i=1}^N X_i \ln X_i, \quad (2.1)$$

it's clear that  $\Delta S_{\text{config}}$  increase with a higher number of constituents in the mix. For instance, the ideal configurational entropy of a binary alloy is  $0.69R$ , while a 5-component alloy is  $1.61R$ . If we neglect other factors that influence the formation of solid solutions (will be covered later), from Gibbs free energy in eq 2.2

$$\Delta G_{\text{mix}} = \Delta H_{\text{mix}} - T\Delta S_{\text{mix}}, \quad (2.2)$$

the two primary factors in formation of solid solution is the mixing enthalpy, which is the driving force to form compounds, and the mixing entropy which is the driving force to form random solid solutions. At elevated temperatures especially, the energy associated to the entropy of the system becomes comparative to the mixing enthalpy and can impact the overall equation. In summary, the overall concept of high-entropy alloys is that through alloying a greater number of elements, the gain in configurational entropy of the system prohibit the formation of intermetallic compounds in favor of a random solid solution. The random term simply relate to the various components occupying lattice positions based on probability. In fact, a narrower definition of high-entropy alloys would be structures with a single-phase disordered solid solution. The two "definitions" given previously can be considered as guidelines for the latter.

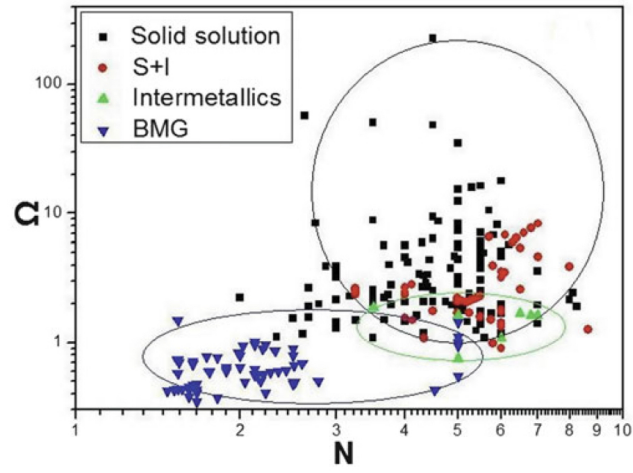
All though the mixing entropy mentioned above plays a central role in the formation, there are other factors to consider, and some that may oppose the formation of a single disordered phase. One of these is the atomic size effect which is related to the differences in atomic size, between the various elements in the alloy, this quantity is denoted  $\delta$ . Y. Zhang et al. in 2008 illustrated the relationship between  $\Delta H_{\text{mix}}$  and  $\delta$ . When  $\delta$  is very small, ie similar atomic sizes. The elements have an equal probability to occupy lattice sites to form solid solutions, but the mixing enthalpy is not negative enough to promote formation of solid solution. Increasing  $\delta$  does result in greater  $\Delta H_{\text{mix}}$ , but leads to a higher degree of ordering. **Include figure?** To summarize the illustration, the formation of solid solution high-entropy alloys occur in a narrow range of  $\delta$  value that satisfy both the enthalpy of mixing and the disordered state. Recently, Yang and Zhang proposed the parameter  $\Omega$  to evaluate the stability of high-entropy alloys. The quantity is a product of the melting temperature  $T_m$ , mixing entropy and mixing enthalpy in the following manner

$$\Omega = \frac{T_m \delta S_{\text{mix}}}{|\Delta H_{\text{mix}}|}. \quad (2.3)$$

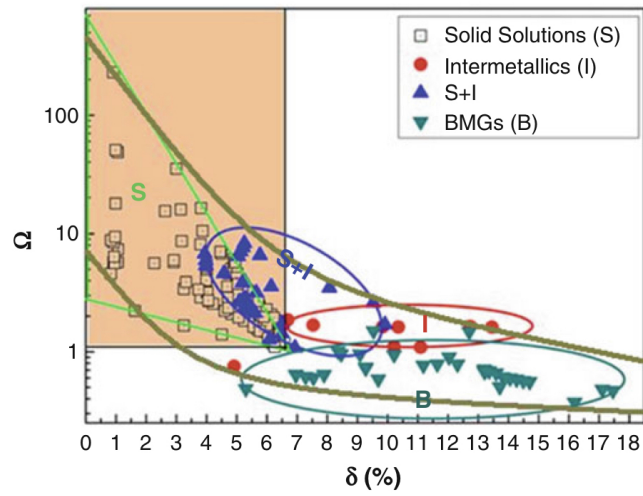
. They managed to obtain a qualitative condition for formation of the single disordered solid solution at  $\Omega \geq 1.1$  and  $\delta \leq 6.6\%$ . While compounds such as intermetallics form for greater values of  $\delta$  and lesser values of  $\Omega$ . Similarly, replacing the atomic size effect constant for the number of elements result in an equivalent condition. The results are summarized in figure 2.1

An important quantity in terms of characterizing high-entropy alloys is the total number of electrons VEC. The valence electron concentration of





(a) HEA formation based on  $\Omega$  and  $\delta$



(b) HEA formation based on  $\Omega$  and  $N$

Figure 2.1: Formation of HEA based on  $\delta$  and  $N$ . Figures adopted from [14]

a material is strongly related to the crystal structure of the material. For example,  $Co_3V$ , originally a hexagonal structure can be transformed into a tetragonal or cubic structure by either increasing the VEC from alloying with Ni, or reduction with Fe respectfully. Derived from the work of Guo et al. on the phase stability of a  $Al_xCrCuFeNi_2$  HEA, the VEC can be directly related to the crystal structure of high-entropy alloys. A lower VEC stabilize the BCC phase, while higher values stabilize FCC. In between is a mixture of the two. Specifically values greater than 8.0 stabilize FCC, and values below 6.87 favor BCC. However, these boundaries are not rigid when including elements outside of transition metals, exceptions have also been found for high-entropy alloys containing Mn. All though a heavy majority of reported high-entropy alloys that form solid solutions have been found to adopt simple cubic structures such as FCC and BCC. Recent studies have observed HEA's in orthorhombic structures like  $Ti_{35}Zr_{27.5}Hf_{27.5}Ta_5Nb_5$  and hcp structures, for example  $CoFeNiTi$ .

## 2.2 Core effects and properties

Next, we will summarize the discussion above into four core elements that distinctly describe high-entropy alloys and their implications on the functional properties. The first of these is the "high-entropy effect", as the name suggests this is related to the increased configurational entropy from the amount of elements, that can inhibit the formation of strongly ordered structures. The second effect is the "severe lattice distortion effect", that originates from the fact that every element in a high-entropy structure is surrounded by non-homogeneous elements, thus leading to severe lattice strain and stress. The overall lattice distortion is additionally attributed to the differences in atomic size, bonding energies and crystal structure tendencies between the components. Therefore the total lattice distortion observed in HEA's are significantly greater than that of conventional alloys. This effect mostly affects the strength and conductivity of the material, such that a higher degree of distortion yields greater strength and greatly reduces the electronic and thermal conductivity due to increased electron and phonon scattering. An upside to this is that the scattering and following properties become less temperature dependent given that it originates from the lattice rather than thermal vibrations.

The two remaining effects, "sluggish diffusion" and "cocktail effect" can be summarized swiftly. The first is a direct consequence of the multi-component layout of high-entropy alloys that result in slowed diffusion and phase transformation because of the number of different elements that is demanded in the process. The most notable product from this effect is an increased creep resistance. Lastly we have the cocktail effect, which is identical to the smoothie analogy mentioned previously, in that the resultant characteristics is a combination of both the elements and their interaction. This is possibly the most promising concept behind high-entropy alloys, which fuels researchers with ambition to discover highly optimized materials by meticulously combining and predicting

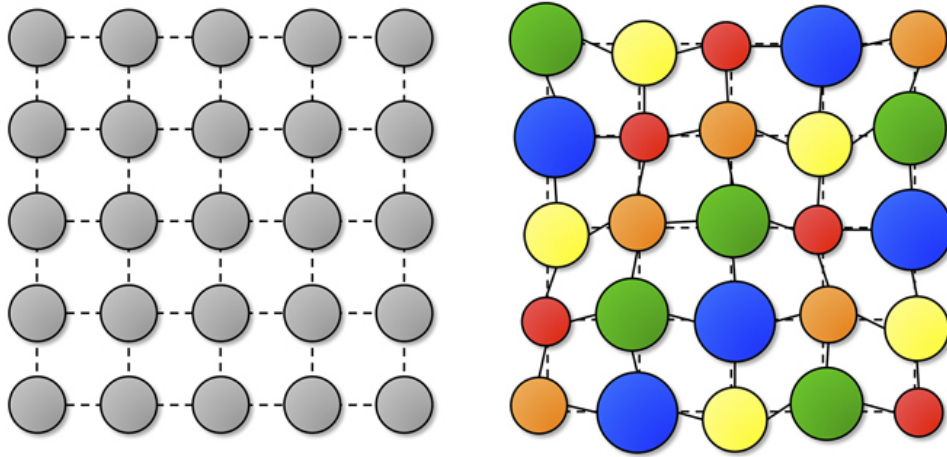


Figure 2.2: A schematic illustration of lattice distortion in high-entropy alloys. Figure from [3]

properties from different elements. Examples of this can be the refractory HEA's developed by "Air Force Research Laboratory" severely exceeding the melting points and strength of previous Ni or Co-based superalloys by alloying specifically refractory elements such as Mo, Nb and W. Another example is the research conducted by Zhang et al. on the high-entropy system  $FeCoNi(AlSi_{0-0.8})$  in the intent of unveiling the optimal combination of magnetic, electric and mechanical properties, resulting in an excellent soft magnet.

In the discussion above, we have covered the four core effects that make up high-entropy alloys and their relation to the mechanical and functional properties. Of the core effects, especially the lattice distortion and cocktail effect relate to the functional properties. The initial study on the functional properties on high-entropy alloys was conducted on the H-x alloy, referring to the system  $Al_xCoCrFeNi$  with  $0 \leq x \leq 2$ . It was found that the electrical resistivity was higher than that of conventional alloys, and that the conductivity generally decreased with increasing amounts of Al, additionally noteworthy low carrier mobility. Similar findings have also been made for the high-entropy alloy  $FeCoNi(AlSi)_x$ .

**Write a small part on magnetic and relate to the cocktail effect, then very briefly conclude by mentioning findings of superconductivity, corrosion resistance, hydrogen storage and other properties/applications.**

## Chapter 3

# Modeling of random alloys

The structure of high-entropy alloys in which the alloying elements occupy lattice sites by a random probability pose a problem on the numerical methods used for modeling. DFT in particular rely heavily on the periodicity in crystalline solids, as we will discover later. In a brute force approach, this could be solved by randomly distribute the solute and solvent atoms over the lattice sites of a large supercell and average the energy and related properties of a great number of such supercells with varying distributions. Obviously this approach is rather efficient or even doable considering the computational demand. Thankfully today there exists a number of possible methods to more efficiently study such structures. Examples are the virtual crystal approximation (VCA), Coherent Potential approximation (CPA), special quasi-random structure (SQS), and hybrid monte-carlo/molecular dynamics. (MC/MD). A brief review of the different models is given in for example [6]. In this project we will employ the SQS method, due to both it's easy to use implementation and interpretation in VASP compared to the other options, and other benefits that will become clear after the following sections.

### 3.1 The Special Quasi-random Structure model

In the original paper on SQS published in 1990 [10], it was proposed a selective occupation strategy to design special periodic quasi-random structures that exceeded previous methods in both accuracy and cost. The key concept was to create a periodic unit cell of the various components in a finite  $N$  lattice site single configuration such that the structure most closely resemble the configuration average of an infinite perfect random alloy. In an attempt to work withing the 50 lattice sites boundary of ab initio methods at that time. The working theory was that if one can resemble an infinite perfect random alloy by a periodic finite  $N$  cell, also the electronic properties would be similar between the two. The solution to this model was that for each  $N$ , ie lattice site, to minimize the difference of structural correlation function between the approximated cell and the perfect random alloy. There are obviously errors involved with approximating a random alloy by a periodic cell, but by the hierarchical relation to the properties of

the material, interactions between distant sites only offer a negligible small contribution to the total energy of the system. Thus the aim of the SQS method is focused around optimizing the correlations within the first few shells of a given site. To follow is a review of the mathematical description of special quasi-random structures.

### 3.1.1 Mathematical description

We begin this section by giving a brief review of topics such as cluster expansions, statistics and superposition of periodic structures. A broader description of these topics can be found in the original article, or elsewhere in the literature. On a side note regarding the following mathematical derivation, the original concept was devolved in mind of an random binary alloy, but the theory have late successfully been extended to multi-component alloys and other special cases.

The different possible atomic arrangements are denoted as "configurations"  $\sigma$ . The various physical properties of a given configuration is  $E(\sigma)$ , and  $\langle E \rangle$  is the ensemble average over all configurations  $\sigma$ . In practice, this quantity is unfeasible in terms of computational cost, seeing as the average require calculations and relaxations of all possible configurations, for a binary alloy this is  $2^N$  for a fixed  $N$  number of lattice sites. A solution to this is to use the theory of cluster expansions and discretize each configuration into "figures"  $f$ . A figure in the lattice is defined in terms of the number of atoms it include  $k$ , distance in terms of neighbors  $m$ , and position in the lattice  $l$ . Further we assign spin values for each lattice site  $i$  in the figure to denote which element it holds (+1,-1 for a binary alloy). By defining the spin product of spin variables in a figure at lattice position  $l$  as  $\Pi_f(l, \sigma)$ , we can write the average of all locations in the lattice of a given figure  $f$  as

$$\Pi_f(\sigma) = \frac{1}{ND_f} \sum_l \Pi_f(l, \sigma) \quad (3.1)$$

where  $D_f$  is the number of equivalent figures  $f$  per site. The brilliance of this notation is that we now can express the physical property  $E(\sigma)$  in terms of the individual contributions  $\epsilon_f$  of a figure  $f$ .

$$E(\sigma) = \sum_{f,l} \Pi_f(l, \sigma) \epsilon_f(l) \quad (3.2)$$

The quantity  $\epsilon_f$  is called the "effective cluster property" and is defined as (for a random binary alloy  $A_{1-x}B_x$ )

$$\epsilon_f(l) = 2^{-N} \sum_{\sigma} \Pi_f(l, \sigma) E(\sigma) \quad (3.3)$$

Inserting the equation for  $\Pi_f$  into that of  $E(\sigma)$  we can describe the the previous cluster expansion of  $E(\sigma)$  as

$$E = N \sum_f D_f \langle \Pi_f \rangle \epsilon_f \quad (3.4)$$

And obtain a simplified expression for  $\langle E(\sigma) \rangle$  in eq 1? Thus we have successfully managed to reduce the expensive task of sampling all  $E(\sigma)$  into calculating the effective cluster properties and summing over all types of figures. Remembering that  $E(\sigma)$  can relate to many physical properties, the most common and applied case is that  $E(\sigma)$  is the total energy, while  $\epsilon_f$  is many body interaction energies. The cluster expansion above converge rather quickly with increasing number of figures, an effective method is thus to select a set of configurations to evaluate the effective cluster properties. Don't know how to write this, but the next step is to select a finite largest figure denoted  $F$ , and "specialize" the cluster expansion to a set of  $N_s$  periodic structures  $\sigma = s$  to obtain the two expressions for  $E(s)$  and  $\epsilon_f$  using matrix inversion to obtain the result for  $\epsilon_f$

$$E(s) = N \sum_f^F D_f \mathbf{\Pi}_f(s) \epsilon_f \quad (3.5)$$

$$\epsilon_f = \frac{1}{ND} \sum_s^{N_s} [\mathbf{\Pi}_f(s)] - 1E(s) \quad (3.6)$$

Assuming now that the sum of figures  $F$  and  $N_s$  periodic structures are well converged,  $E(\sigma)$  can be rewritten as a superposition of  $E(s)$

$$E(\sigma) = \sum_s^{N_s} \zeta_s(\sigma) E(s) \quad (3.7)$$

$$\zeta_s(\sigma) = \sum_f^F [\mathbf{\Pi}_f(s)]^{-1} \mathbf{\Pi}_f(\sigma) \quad (3.8)$$

where  $\zeta$  is the weights. Thus we have effectively reduced the problem to a convergence problem of the number of figures  $F$  and structures  $N_s$ . This can be easily solved given that we are dealing with periodic crystal structures  $s$  that can employ the general applications of ordered structures from ab initio methods, and increasing  $F$  until the truncation error falls below a desired threshold. However, this approach requires that the variance of the observable property is much lower than the sample mean, otherwise one would have to employ a much bigger sample size to reach statistical convergence. Don't how to write this part nicely, but: Because of the different relationship between various physical properties and the correlation functions, one observe different convergence depending on the meaning of  $E$ . The idea behind SQS was therefore to design single special structures with correlation functions  $\mathbf{\Pi}_f(s)$  that most accurately match those of the ensemble average of a random alloy  $\langle \mathbf{\Pi}_f \rangle_R$ .

The correlation functions of an perfect random infinite alloy, denoted as  $R$  is defined below

$$\mathbf{\Pi}_{k,m}(R) = \langle \mathbf{\Pi}_{k,m} \rangle_R = (2x - 1)^l \quad (3.9)$$

with  $k, m$  defined as before and  $x$  being the composition ratio of the alloy. In the case of an eqvimolar alloy ( $x = \frac{1}{2}$ ), the functions equal 0 for all  $k$

except  $\langle \Pi_{0,1} \rangle_R = 1$ . If we now randomly assign either atom A or B to every lattice site, for a sufficiently large value of  $N$ , the goal is then to create a single configuration that best match the random alloy. Keeping with the  $x = \frac{1}{2}$  case, the problem is now that even though the average correlation functions of a large set of these structures approaches zero, like for the random alloy. The variance of the average is nonzero meaning that a selected structure of the sample is prone to contain errors. The extent of these errors can be evaluated from the standard deviations

$$\nu_{k,m}(N) = | \langle \Pi_{k,m}^2 \rangle |^{\frac{1}{2}} = (D_{k,m}N)^{-\frac{1}{2}} \quad (3.10)$$

Given the computational aspects, it's obvious that economical structures with small  $N$  are prone to large errors. In fact, in some cases these errors can result in correlation functions centering around 1, as opposed to 0 for a perfect random alloy.

I don't know how to write the prelude to this part! (see section IIIA in [10]). The degree to which a structure  $s$  fails to reproduce the property  $E$  of the ensemble-averaged property of the random alloy can be described by a hierarchy of figures, see eq .. bellow

$$\langle E \rangle - E(s) = \sum_{k,m}' D_{k,m} [(2x-1)^k - \Pi_{k,m}(s)] \epsilon_{k,m} \quad (3.11)$$

, the prime is meant symbolize the absence of the value 0, 1 for  $k, m$ . The contribution from the figure property  $\epsilon$  reduces for larger figures. In general, for disordered systems, the physical property "E" at a given point  $R$  falls off exponentially as  $|R - R'|/L$ , where  $L$  is a characteristic length scale relating to the specific property. Using this, the approach of SQS is to specify a set of correlation functions that hierarchically mimic the correlation functions of the random alloy. Meaning that it prioritize the nearest neighbor interactions. With the set of functions decided on, the objective is finally to locate the structures that correspond to the selected structures.

With this approach, [10] managed by mimicking the correlation functions exact for the first two shells, to reduce the computational measures of an accurate models. In this exact study they matched the results of an  $N \rightarrow \infty$  by an  $N = 8$  SQS. In the final section of this chapter, we will take a look at the recent advances in the SQS method and application to high-entropy alloys.

### 3.1.2 Applications to high-entropy alloys

The success of the SQS method is in large part related to the fact that we can create simple periodic structures, this allows for the use of standard DFT methods to calculate properties such as the total energy, charge density and electronic band structure [2], [8]. However, some additional challenges are involved when applying the SQS method to model multi-component random alloys such as HEAs. Several of these are covered in the work of M.C Gao et al. [1], whom in 2016 presented a comprehensive

review on high-entropy alloys modeling with SQS in the framework of DFT and VASP.

The first initial concern with applying SQS to model high-entropy alloys is the size of the supercell. This parameter needs to be balanced between accuracy and cost. A larger SQS cell consisting of a greater number of atoms better encapsulate the disordered structure of HEAs, but both the generation and simulation of such large SQSs come with an increased computational demand. An example of this can be seen in the study by M.C Gao et al study on the stability and predicted crystal structure of CoCrFeNi and CoCrFeMnNi HEAs with SQSs of different size. Experimentally both of these is found stable in the FCC structure. By calculating the enthalpy of formation, he found that SQSs under 64 atoms wrongly predicted the HCP structure as the most stable, while larger SQS correctly agreed on the FCC structure. Additionally, the probability distribution functions (PDFs) of the respective SQSs display a dependence to the SQS size. For example in 3 SQSs of size 20, 125 and 250 atoms each of FCC CrFeMnNi, the Cr-Mn is much better represented in the large SQS model as seen bellow in figure 4.1.

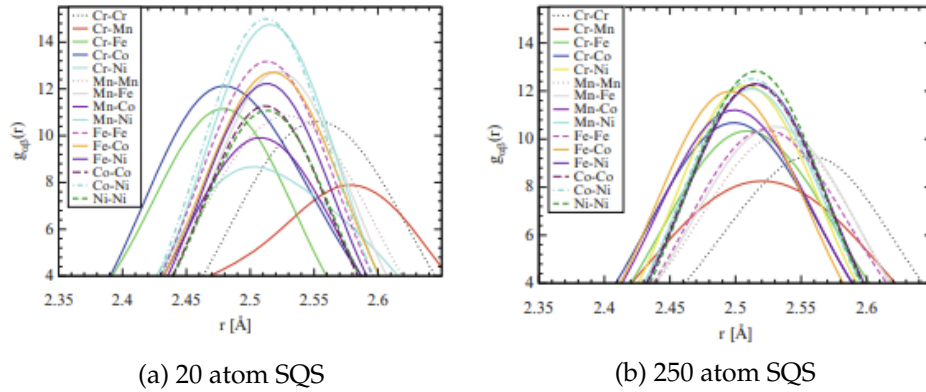


Figure 3.1: PDFs of (a) 20 and (b) 250 atom SQS models of CrFeMnNi [1]

It can also be noted that a similar dependence on the SQS size is apparent for the entropy and mechanical properties, however these topics are not relevant for this project and will thus not be elaborated further.

#### Compare SQS to CPA and MCMD



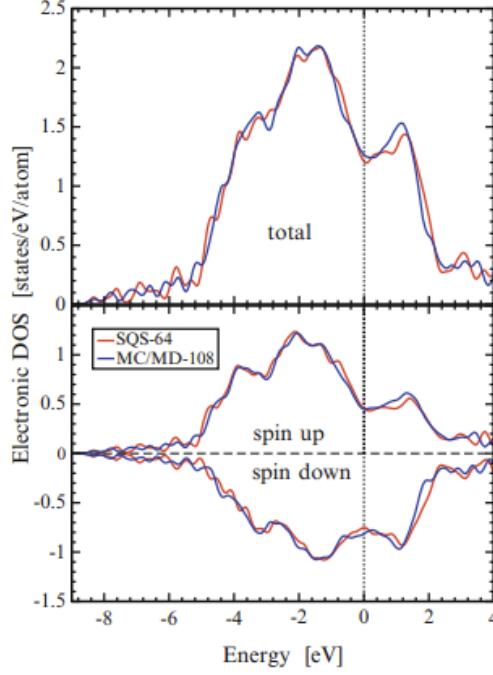


Figure 3.2: Density of states with SQS and MC/MD of FCC CoCrFeNi, figure from [1]

Above ... DOS in agreement between much more complex MC/MD computations of a 108 atom cell and a simple 64 atom SQS. Both these are in agreement but also in disagreement with the DOS from CPA should be noted. But I think the two above is the most accurate.

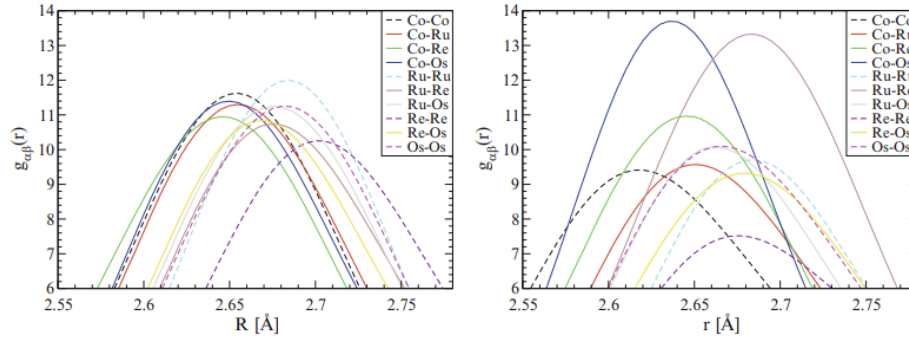


Figure 3.3: Probability distribution functions with SQS and MC/MD of HCP CoOsReRu [1]

The PDFs are more accurate from MCMD due to the inclusion of interatomic interaction that SQS neglect, and is the preferred tool for a larger temperature relation study. But SQS offer excellent result for such simple implementation in comparison. This is illustrated in figure [ABOVE] for the HCP CoOsreRu alloy, in which clear preference of Co-Os and Re-Ru pairs is apparent from MC/MD simulations but not in the SQS.

A significant concern of SQSs is the large number of possible configur-

ations of a alloy. For example a quaternary and quinary alloy respectively offer 24 and 124 unique atomic configurations. In [1] it was found varying sensitivity in the enthalpy of formation to the atomic configuration in different alloys. It was found that the sensitivity is large for anisotropic lattices such as HCP and chemically dissimilar constituents, furthermore a larger SQS size helps to reduce the sensitivity. A final limitation of SQSs is the ability to model specific compositions such as  $A_{1/3}BCDE$  compared to CPA. Additionally both MC/MD and SQS struggle with magnetic materials in general and particularly paramagnets, being more computationally heavy than CPA. Also for large SQSs, the elastic properties can be cumbersome to calculate.

#### **mc-SQS and advances and recent studies.**

up until the use of mcsqs the use of SQS to HEA have been very limited, with most applications lying **How to I write this final paragraph of why SQS is used at HEAs today? mcSQS?** Something on in very recent time, computational resources have increased and the generation of SQS have improved by the mc-SQS approach? This allows for a reduction in cell size and computation time, all though the convergence of SQSs and magnetic configuration remain troublesome in some cases. Maybe mention that the implementation of the TDEP package drastically improve the computational cost.

application to high-entropy alloys have been limited prior to the last couple of years on the grounds of computational demands involved in modeling disordered multi-component systems and the very recent emergence of the field in general. Mainly the last few years have we seen studies of high-entropy alloys based on special quasi-random structures [7], [9], [4], [5].

**Part II**

**Methodology and  
Implementation**

**Part III**

**Results and Discussion**

**Part IV**

**Conclusion**

Write conclusion here

# Bibliography

- [1] Michael C. Gao et al. 'Applications of Special Quasi-random Structures to High-Entropy Alloys'. In: *High-Entropy Alloys: Fundamentals and Applications*. Ed. by Michael C. Gao et al. Cham: Springer International Publishing, 2016, pp. 333–368. ISBN: 978-3-319-27013-5. DOI: 10.1007/978-3-319-27013-5\_10. URL: [https://doi.org/10.1007/978-3-319-27013-5\\_10](https://doi.org/10.1007/978-3-319-27013-5_10).
- [2] Z. W. Lu, S.-H. Wei and Alex Zunger. 'Electronic structure of ordered and disordered  $\text{Cu}_3\text{Au}$  and  $\text{Cu}_3\text{Pd}$ '. In: *Phys. Rev. B* 45 (18 May 1992), pp. 10314–10330. DOI: 10.1103/PhysRevB.45.10314. URL: <https://link.aps.org/doi/10.1103/PhysRevB.45.10314>.
- [3] Lewis Robert Owen and Nicholas Gwilym Jones. 'Lattice distortions in high-entropy alloys'. In: *Journal of Materials Research* 33.19 (2018), pp. 2954–2969. DOI: 10.1557/jmr.2018.322.
- [4] Muhammad Rashid et al. 'Ab-initio study of fundamental properties of ternary  $\text{ZnO}_{1-x}\text{S}_x$  alloys by using special quasi-random structures'. In: *Computational Materials Science* 91 (2014), pp. 285–291. ISSN: 0927-0256. DOI: <https://doi.org/10.1016/j.commatsci.2014.04.032>. URL: <https://www.sciencedirect.com/science/article/pii/S0927025614002742>.
- [5] V. Sorkin et al. 'First-principles-based high-throughput computation for high entropy alloys with short range order'. In: *Journal of Alloys and Compounds* 882 (2021), p. 160776. ISSN: 0925-8388. DOI: <https://doi.org/10.1016/j.jallcom.2021.160776>. URL: <https://www.sciencedirect.com/science/article/pii/S092583882102185X>.
- [6] Fuyang Tian. 'A Review of Solid-Solution Models of High-Entropy Alloys Based on Ab Initio Calculations'. In: *Frontiers in Materials* 4 (2017). ISSN: 2296-8016. DOI: 10.3389/fmats.2017.00036. URL: <https://www.frontiersin.org/article/10.3389/fmats.2017.00036>.
- [7] Shen Wang et al. 'Comparison of two calculation models for high entropy alloys: Virtual crystal approximation and special quasi-random structure'. In: *Materials Letters* 282 (2021), p. 128754. ISSN: 0167-577X. DOI: <https://doi.org/10.1016/j.matlet.2020.128754>. URL: <https://www.sciencedirect.com/science/article/pii/S0167577X20314610>.
- [8] Su-Huai Wei and Alex Zunger. 'Band offsets and optical bowings of chalcopyrites and Zn-based II-VI alloys'. In: *Journal of Applied Physics* 78.6 (1995), pp. 3846–3856. DOI: 10.1063/1.359901. eprint: <https://doi.org/10.1063/1.359901>. URL: <https://doi.org/10.1063/1.359901>.

- [9] Peng Wei et al. 'Understanding magnetic behaviors of FeCoN<sub>i</sub>Si<sub>0.2</sub>M<sub>0.2</sub> (M=Cr, Mn) high entropy alloys via first-principle calculation'. In: *Journal of Magnetism and Magnetic Materials* 519 (2021), p. 167432. ISSN: 0304-8853. DOI: <https://doi.org/10.1016/j.jmmm.2020.167432>. URL: <https://www.sciencedirect.com/science/article/pii/S0304885320323994>.
- [10] S.-H. Wei et al. 'Electronic properties of random alloys: Special quasirandom structures'. In: *Phys. Rev. B* 42 (15 Nov. 1990), pp. 9622–9649. DOI: 10.1103/PhysRevB.42.9622. URL: <https://link.aps.org/doi/10.1103/PhysRevB.42.9622>.
- [11] Jien-Wei Yeh. 'Overview of High-Entropy Alloys'. In: *High-Entropy Alloys: Fundamentals and Applications*. Ed. by Michael C. Gao et al. Cham: Springer International Publishing, 2016, pp. 1–19. ISBN: 978-3-319-27013-5. DOI: 10.1007/978-3-319-27013-5\_1. URL: [https://doi.org/10.1007/978-3-319-27013-5\\_1](https://doi.org/10.1007/978-3-319-27013-5_1).
- [12] Jien-Wei Yeh. 'Physical Metallurgy'. In: *High-Entropy Alloys: Fundamentals and Applications*. Ed. by Michael C. Gao et al. Cham: Springer International Publishing, 2016, pp. 51–113. ISBN: 978-3-319-27013-5. DOI: 10.1007/978-3-319-27013-5\_3. URL: [https://doi.org/10.1007/978-3-319-27013-5\\_3](https://doi.org/10.1007/978-3-319-27013-5_3).
- [13] Jien-Wei Yeh et al. 'Functional Properties'. In: *High-Entropy Alloys: Fundamentals and Applications*. Ed. by Michael C. Gao et al. Cham: Springer International Publishing, 2016, pp. 237–265. ISBN: 978-3-319-27013-5. DOI: 10.1007/978-3-319-27013-5\_7. URL: [https://doi.org/10.1007/978-3-319-27013-5\\_7](https://doi.org/10.1007/978-3-319-27013-5_7).
- [14] Yong Zhang et al. 'Phase Formation Rules'. In: *High-Entropy Alloys: Fundamentals and Applications*. Ed. by Michael C. Gao et al. Cham: Springer International Publishing, 2016, pp. 21–49. ISBN: 978-3-319-27013-5. DOI: 10.1007/978-3-319-27013-5\_2. URL: [https://doi.org/10.1007/978-3-319-27013-5\\_2](https://doi.org/10.1007/978-3-319-27013-5_2).